Comparative DFT Study of Crystalline Ammonium Perchlorate and Ammonium Dinitramide

Weihua Zhu,* Tao Wei, Wei Zhu, and Heming Xiao*

Institute for Computation in Molecular and Materials Science and Department of Chemistry, Nanjing University of Science and Technology, Nanjing 210094, China

Received: January 21, 2008; Revised Manuscript Received: February 27, 2008

The electronic structure, vibrational properties, absorption spectra, and thermodynamic properties of crystalline ammonium perchlorate (AP) and ammonium dinitramide (ADN) have been comparatively studied using density functional theory in the local density approximation. The results shows that the p states for the two solids play a very important role in their chemical reaction. From the low frequency to high frequency region, ADN has more motion modes for the vibrational frequencies than AP. The absorption spectra of AP and ADN display a few, strong bands in the fundamental absorption region. The thermodynamic properties show that ADN is easier to decompose than AP as the temperature increases.

1. Introduction

Ammonium perchlorate (AP), NH_4ClO_4, has its widespread use in solid rocket propellants because it is cheap and contains a large amount of oxygen that is converted entirely into stable gaseous products during combustion.[1–3] However, since AP produces HCl gas as a combustion product, there is considerable interest in finding environmentally benign replacements for the energetic oxidizer AP. Ammonium dinitramide (ADN), $NH_4N(NO_2)_2$, has been identified as a promising energetic candidate and is, to some extent, serving as the prototypical dinitramide salt.[4–7] It is a powerful oxidizer without the environmental problems of AP. Therefore, understanding the differences between the fundamental properties of the two solids is important for the development of new propellants.

A desire to probe more fundamental questions relating to the basic properties of the two salts as solid energetic materials is generating significant interest in the basic solid-state properties of such energetic systems. The electronic structure is intimately related to their fundamental physical and chemical properties; moreover, an understanding of electronic structure and properties is necessary for discussion of electronic processes as they relate to decomposition and initiation. On the other hand, although the detailed decomposition mechanism by which the two solids releases energy under mechanical shock is still not well understood, it has been suggested that their decomposition may result from transferring thermal and mechanical energy into the internal degrees of freedom of tightly bonded groups of atoms in solid. Therefore, the knowledge of its electronic structure and properties appears to be very important in understanding its explosive properties.

The investigation of the microscopic properties of energetic materials, which possess a complex chemical behavior, remains to be a challenging task. Theoretical calculations are an effective way to model the physical and chemical properties of complex solids at the atomic level as a complement to experimental work. Recently, the density functional theory (DFT) method with pseudopotentials and a plane-wave basis set has been well-established and has been successfully applied to the study of structures and properties of solids. Sorescu and Thompson[8] have studied the structural properties of ADN crystal at ambient pressure by using DFT with pseudopotentials. Afterward, they used the same method to investigate the structural properties of crystalline ADN under hydrostatic compression in the pressure range 0–300 GPa.[9] As the electronic structure and properties of the two solid are not systematically compared, there is a clear need to gain an understanding of those at the ab initio level.

In this study, we performed periodic density functional theory (DFT) calculations to study the electronic structure, vibrational properties, absorption spectra, and thermodynamic properties of AP and ADN. Our main purpose here is to examine the differences in the electronic structure and properties among them.

The remainder of this paper is organized as follows. A brief description of our computational method is given in section 2. The results and discussion are presented in section 3, followed by a summary of our conclusions in section 4.

2. Computational Method

The calculations performed in this study were done within the framework of DFT,[10] using Vanderbilt-type ultrasoft pseudopotentials[11] and a plane-wave expansion of the wave functions. The self-consistent ground state of the system was determined by using a band-by-band conjugate gradient technique to minimize the total energy of the system with respect to the plane-wave coefficients. The electronic wave functions were obtained by a density-mixing scheme,[12] and the structures were relaxed by using the Broyden, Fletcher, Goldfarb, and Shannon (BFGS) method.[13] The local density approximation (LDA) functional proposed by Ceperley and Alder[14] and parameterized by Perdew and Zunder,[15] named CA-PZ, was employed. The cutoff energy of plane waves was set to 600.0 eV. Brillouin zone sampling was performed by using the Monkhost−Pack scheme with a k point grid of $3 \times 3 \times 3$. The values of the kinetic energy cutoff and the k point grid were determined to ensure the convergence of total energies.

AP crystallizes in an orthorhombic $Pna2_1$ space group and contains four molecules per unit cell.[16] Each perchlorate ion is surrounded by seven ammonium ions, and vice versa. ADN

* To whom correspondence should be addressed. Fax: +86-25-84303919. E-mail: zhuwh@mail.njust.edu.cn (W.Z.), xiao@mail.njust.edu.cn (H.X.).

10.1021/jp800693e CCC: $40.75
Published on Web 04/09/2008

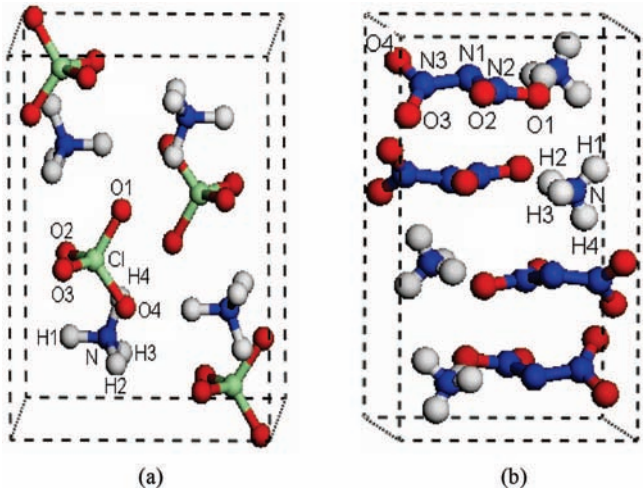

Figure 1. Unit cells for (a) AP and (b) ADN.

crystallizes in a monoclinic space group, $P2_1/c$, with four molecules per unit cell. There is strong hydrogen bonding involving all four ammonium hydrogen atoms with the oxygen atoms of the surrounding dinitramide ions. The crystal structure of ADN at ambient pressure has been resolved by X-ray diffraction measurements.[17] The crystal structures of AP and ADN are shown in Figure 1.

Starting from the above-mentioned experimental structures, the geometry relaxation was performed to allow the ionic configurations, cell shape, and volume to change. In the geometry relaxation, the total energy of the system was converged less than 2.0×10^{-5} eV, the residual force less than 0.05 eV/Å, the displacement of atoms less than 0.002 Å, and the residual bulk stress less than 0.1 GPa. For all of the relaxed structures, the Mulliken charges and bond populations were investigated using a projection of the plane-wave states onto a linear combination of atomic orbitals (LCAO) basis set,[18,19] which is widely used to perform charge transfers and populations analysis. The phonon frequencies at the gamma point have been calculated from the response to small atomic displacements.[20]

3. Results and Discussion

3.1. Bulk Properties. The calculated cell parameters, bond lengths, and bond angles of AP and ADN are given in Table 1 together with their experimental results.[16,17] The calculated results reproduce the measured cell parameters of AP and ADN. The differences between the calculated and the experimental values are typical for the LDA approximation to DFT. We also note that the calculated bond lengths and bond angles are very close to the corresponding experimental data except for the N−O bond lengths. These comparisons confirm that our computational parameters are reasonably satisfactory.

3.2. Electronic Structure. The calculated total density of states (DOS) and partial DOS (PDOS) for AP and ADN are displayed in Figures 2 and 3, respectively. Clearly, the structures are very similar except some subtle differences. The DOS of the two solids are finite at the Fermi energy level. This is because the DOS contain some form of broadening effect. In the upper valence band, both AP and ADN have a sharp peak near the Fermi level. The top of the DOS valence band shows two main peaks for AP, and three main peaks for ADN. These peaks are predominately from the p states. After that, several main peaks in the upper valence band are superimposed by the s and p states. The conduction band is dominated by the p states. This indicates that the p states for the two solids play a very important role in their chemical reaction.

TABLE 1: Experimental (in Parentheses) and Relaxed Cell Parameters, Bond Lengths (Å), and Bond Angles (Degree) for Crystalline AP and ADN

AP			ADN		
	this work	expt[16]		this work	expt[17]
Cell Parameter					
a(Å)	9.344	9.227	a(Å)	6.98	6.914
b(Å)	7.302	7.454	b(Å)	12.121	11.787
c(Å)	6.309	5.819	c(Å)	5.416	5.614
			β(deg)	99.15	100.40
Bond Length					
Cl−O1	1.437	1.441	N1−N2	1.359	1.376
Cl−O2	1.438	1.452	N1−N3	1.359	1.359
Cl−O3	1.426	1.426	N2−O1	1.261	1.236
Cl−O4	1.433	1.435	N2−O2	1.249	1.227
			N3−O3	1.272	1.252
			N3−O4	1.241	1.223
Bond Angle					
O1−Cl−O2	109.3	108.8	N2−N1−N3	114.8	113.2
O1−Cl−O3	109.2	108.6	O1−N2−O2	123.9	123.3
O1−Cl−O4	109.5	110.4	O1−N2−N1	113.0	113.0
O2−Cl−O3	110.0	110.9	O2−N2−N1	122.8	123.3
O2−Cl−O4	108.8	107.4	O3−N3−O4	122.3	122.1
O3−Cl−O4	109.8	110.7	O3−N3−N1	112.6	114.4
			O4−N3−N1	124.7	125.1

The atom-resolved DOS and PDOS of AP and ADN are also shown in Figures 2 and 3, respectively. The main features can be summarized as follows. (i) In the upper valence band, the PDOS of the states of O are far larger than that of the states of Cl and N. It is expected that the states of O make more important contributions to the valence bands than those of Cl and N. This shows that O in AP and ADN acts as an active center. (ii) For AP, some strong peaks occur at the same energy in the PDOS of a particular Cl atom and a particular O atom. It can be inferred that the two atoms are strongly bonded. Similarly, for ADN, a particular N atom of $N_3O_4^-$ and a particular O atom are strongly bonded. (iii) There are some differences in the PDOS of the O atoms for AP and ADN. This is due to the differences in their local molecular packing. The same is true of the N atoms of NH_4^+. (iv) In the conduction band region of DOS, the peaks of AP are dominated by the Cl p states and O p states, while these

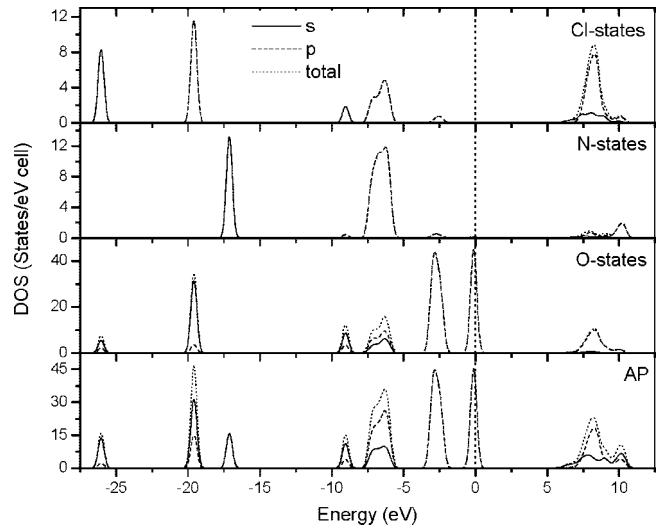

Figure 2. Total and partial density of states (DOS) of Cl states, N states, O states, and AP. The Fermi energy is shown as a dashed vertical line.

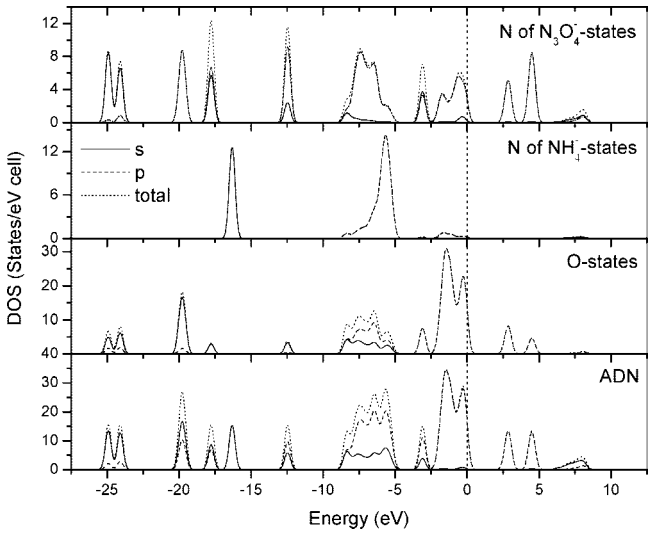

Figure 3. Total and partial density of states (DOS) of N of $N_3O_4^-$ states, N of NH_4^+ states, O states, and ADN.

of ADN are from the N p states of $N_3O_4^-$ and O p states. (v) In the energy range from −5.0 to 0 eV, the DOS of AP are superimposed by the Cl states and O states, whereas that of ADN mainly arises from the N states of amide and NO_2. It may be inferred that the Cl−O bonds in AP, first, may be broken in the decomposition of AP. This is consistent with the previous report[21] that the Cl−O bond scission reaction for AP would be favorable in the crystalline phase. For ADN, the N−N bond fission reactions are more favorable than other bond fissions. Vyazovkin and Wight[22] have used differential scanning calorimetry and thermal gravimetry combined with mass spectrometry to study thermal decomposition of ADN and proposed that condensed phase ADN may decompose by an initial step that involves N−N bond scission. This further supports our conclusion here.

The electronic structure can be further analyzed by examining the charge transfer and bond order in AP and ADN. The Mulliken charge and overlap population are useful in evaluating the nature of bonds in a compound. Although the absolute magnitudes of Mulliken populations have little physical meaning, the relative values can still offer some useful information. Table 2 shows the charge transfer and bond order values for AP and ADN. The charge transfer from H to N in AP is 1.06 e, close to 1.04 e in ADN. This similarity can actually be seen from the PDOS of Figures 2 and 3 where the N 4p peak is at about the same energy in AP and ADN. The effective charge of the O atom ranges from 0.86 to 0.88 in AP and from 0.39 to 0.42 in ADN. These differences reflect the different types of oxygen bonding. The O in AP is bonded to Cl atom, while the O in ADN is to N atoms. The effective charge of NH_4^+ ions in AP is 0.86, while that in ADN is 0.76, showing that the NH_4^+ ions in AP and ADN are in different local packing. So we may conclude that the AP crystal has stronger ionic bonding than ADN.

Bond order is a measure of the overall bond strength between two atoms. A high value of the bond order indicates a covalent bond, while a low value shows an ionic nature. The bond orders of the N−H bonds are from 0.60 to 0.61 in AP and from 0.59 to 0.62 in ADN, indicating that the N−H bonds in the two crystals are in different local packing. Therefore, the bond orders are affected by the presence of other nearby atoms or bond angles, not just the two atoms that form a bond. The bond orders of the four Cl−O bonds are nearly equal. This shows the similar

TABLE 2: Calculated Charge Transfers (e) and Bond Order for Crystalline AP and ADN

AP		ADN	
	Charge Transfer		
N	1.06	N	1.04
H	−0.48	H	−0.45
Cl	−2.62	N1	0.19
O1	0.86	N2	−0.50
O2	0.87	N3	−0.51
O3	0.87	O1	0.42
O4	0.88	O2	0.37
		O3	0.40
		O4	0.39
	Bond Order		
N−H1	0.60	N−H1	0.59
N−H2	0.61	N−H2	0.59
N−H3	0.61	N−H3	0.60
N−H4	0.61	N−H1	0.62
Cl−O1	0.42	N1−N2	0.66
Cl−O2	0.43	N2−N3	0.67
Cl−O3	0.43	N2−O1	0.66
Cl−O4	0.43	N2−O2	0.75
		N3−O3	0.69
		N3−O4	0.74

types of local Cl−O bonding. The N1−N2 bond has bond order value of 0.66, very close to the N2−N3 bond order of 0.67. This shows that the N1−N2 and N2−N3 bonds have similar bond strength. The bond orders of the N2−O1 and N2−O2 bonds are not equal, reflecting the two bonds are in different local packing. The same is true of the N3−O3 and N3−O4 bonds.

3.3. Vibrational Properties. The vibrational frequencies for solid AP and ADN are investigated here. Both the internal modes due to intramolecular interactions and the lattice modes due to intermolecular interactions were considered here. Table 3 presents the calculated vibrational frequencies for AP and ADN together with the experimental values.[23–25] The results show that the calculated and measured frequencies are in reasonable agreement. We should note that our calculations are performed at zero temperature but the experimental measures were recorded at low temperature (17, 298.13, and 296 K), so the direct comparison between the calculated and the measured data will result in the discrepancies.

The lattice mode spectra of AP and ADN display similar features in the region 28–220 cm^{-1}. AP has seven frequencies in this region, which are in good agreement with the experimental reports,[24] whereas the lattice mode spectra of ADN were not reported by the experiments. The modes of 103.7 and 115.2 cm^{-1} in ADN correspond to the twist of NO_2 about the N−N bond. The 260.1 and 320.2 cm^{-1} modes corresponding to the lattice vibration appear in ADN but not in AP. In the region of 400–700 cm^{-1}, AP has 4 frequencies. The molecular motion of the first frequency is the symmetric bending of ClO_4, and the motions corresponding to the following frequencies are concentrated in the asymmetric bending of ClO_4. Similarly, ADN also has four frequencies. The molecular motion of the first frequency is the symmetric bending of $N(NO_2)_2$, and the motions corresponding to the following frequencies are concentrated in the asymmetric bending of $N(NO_2)_2$. The modes of 739.7, 822.1, and 938.4 cm^{-1} in ADN, which do not appear in AP, correspond to the asymmetric bending of $N(NO_2)_2$. The calculated frequency 739.7 cm^{-1} for ADN is consistent with the experimental value 739.0 cm^{-1}.[25]

In the region of 1000–1200 cm^{-1}, AP has 5 frequencies. The molecular motions of the first two frequencies are the symmetric

TABLE 3: Vibrational Frequencies (cm^{-1}) for Crystalline AP and ADN

AP					ADN		
	Raman						
this work	ref 23	ref 24	IR[23]	assignment	this work	Raman[25]	assignment
29.6		28.0		lattice vibration	41.3		lattice vibration
61.4		60.0		lattice vibration	61.7		lattice vibration
80.0		81.0		lattice vibration	80.0		lattice vibration
					103.7		twist of NO_2 about NN bond
					115.2		twist of NO_2 about NN bond
144.3		140.0		lattice vibration	146.4		lattice vibration
153.1		158.0		lattice vibration	154.5		lattice vibration
196.8		199.0		lattice vibration	195.4		lattice vibration
215.9		220.0		lattice vibration	218.1		lattice vibration
					260.1		lattice vibration
					320.2		lattice vibration
463.5	463.0	465.0		ClO_4 symmetric bend	463.1		$N(NO_2)_2$ symmetric bend
606.5	627.0	627.0	627.0	ClO_4 asymmetric bend	525.7		$N(NO_2)_2$ asymmetric bend
614.5	632.0	632.0		ClO_4 asymmetric bend	611.7		$N(NO_2)_2$ asymmetric bend
615.0	637.0	637.0	637.0	ClO_4 asymmetric bend	615.6		$N(NO_2)_2$ asymmetric bend
					739.7	739.0	$N(NO_2)_2$ asymmetric bend
					822.1		$N(NO_2)_2$ asymmetric bend
					938.4		$N(NO_2)_2$ asymmetric bend
1048.5	922.0	921.5		ClO_4 symmetric stretch	1045.1		$N(NO_2)_2$ symmetric stretch
1048.6	937.0	936.5	937.0	ClO_4 symmetric stretch	1047.6		$N(NO_2)_2$ symmetric stretch
1053.7	1078.0	1063.0	1078.0	ClO_4 asymmetric stretch	1049.8		$N(NO_2)_2$ asymmetric stretch
1054.1	1109.0	1107.0	1110.0	ClO_4 asymmetric stretch	1050.8		$N(NO_2)_2$ asymmetric stretch
1190.1	1133.0	1133.0	1134.0	ClO_4 asymmetric stretch	1154.2	1174.0	NO_2 symmetric stretch
					1292.6		NO_2 symmetric stretch
					1311.8		NO_2 symmetric stretch
1412.6	1410.0	1427.0	1410.0	NH_4 asymmetric bend	1426.3		NH_4 asymmetric bend
					1706.6		NO_2 asymmetric stretch
					1708.5		NO_2 asymmetric stretch
3212.8	3212.5	3206.0		NH_4 symmetric stretch	3116.2		NH_4 symmetric stretch
3278.6	3267.0	3262.0	3268.0	NH_4 asymmetric stretch	3187.4		NH_4 asymmetric stretch

stretching of ClO_4, and the motions corresponding to the following frequencies are the asymmetric bending of ClO_4. The calculated frequencies for AP in this region have large deviations from the corresponding experimental values. The motions of these frequencies are concentrated in the ClO_4 moieties, thus this discrepancy may be due to intermolecular hydrogen bonding interactions present in the crystal lattice, which are not well-described by DFT. ADN also has five frequencies in this region. The molecular motions of the first two frequencies are the symmetric stretching of $N(NO_2)_2$; the motions corresponding to the following two frequencies are the asymmetric bending of $N(NO_2)_2$, and the motion to the last frequency 1154.2 cm^{-1}, which agrees with the experimental value,[25] is the symmetric stretching of NO_2. The modes of 1292.6 and 1311.8 cm^{-1} in ADN correspond to the symmetric stretching of NO_2. In the region of 1400–3300 cm^{-1}, the motion modes of NH_4 in AP and ADN present similar features. The motion of the first frequency involves the asymmetric bending of NH_4, whereas those of the next two frequencies are concentrated in the symmetric and asymmetric stretching of NH_4, respectively. The modes of 1706.6 and 1708.5 cm^{-1} in ADN correspond to the asymmetric stretching of NO_2.

From the low frequency to high frequency region, ADN has more motion modes for the vibrational frequencies than AP. The motions of the NO_2 groups in ADN are diffusely distributed. Since the torsional motions of the molecule's functional groups are usually supposed to be highly coupled to the other moiety of the molecule,[26] it is possible that the torsion motions of the NO_2 groups act as doorways through which kinetic energy can flow into the molecule from its surroundings. These suggestions show that the NO_2 groups play a very important role in the decomposition of ADN.

3.4. Absorption Spectra. In this section, we turn to investigate the optical absorption coefficients of AP and ADN. The interaction of a photon with the electrons in the system can result in transitions between occupied and unoccupied states. The spectra resulting from these excitations can be described as a joint density of states between the valence and the conduction bands. The imaginary part $\varepsilon_2(\omega)$ of the dielectric function can be obtained from the momentum matrix elements between the occupied and unoccupied wave functions within the selection rules, and the real part $\varepsilon_1(\omega)$ of dielectric function can be calculated from the imaginary part $\varepsilon_2(\omega)$ by the Kramer−Kronig relationship. Absorption coefficient $\alpha(\omega)$ can be evaluated from $\varepsilon_1(\omega)$ and $\varepsilon_2(\omega)$.[27]

$$\alpha(\omega) = \sqrt{2}\omega\left(\sqrt{\varepsilon_1^2(\omega) + \varepsilon_2^2(\omega)} - \varepsilon_1(\omega)\right)^{1/2} \quad (1)$$

The absorption coefficient $\alpha(\omega)$ of AP and ADN are plotted in Figure 4. The absorption spectra are active over various regions corresponding to the molecular or lattice structures of the individual materials. The evolution pattern of absorption spectra for the AP and ADN crystals is qualitatively similar. Both exhibit a relatively high absorption coefficient over a relatively few, narrow bands, typical of ionic salts. The absorption coefficient of the band at 10.6 μm for AP is estimated by our calculations to be 197.02 cm^{-1}, very close to the measured absorption coefficient of 191 cm^{-1} at the same wavelength.[28] We note that the two crystals have a absorption band covering from 0 to 30.0 eV and more strong optical absorption from 3.0 to 20.0 eV. There are five absorption peaks in $\alpha(\omega)$ spectra of them. The magnitude of the absorption coefficients of these peaks allows an optical transition due to excitons. In the absorption spectra of AP, the absorption peak

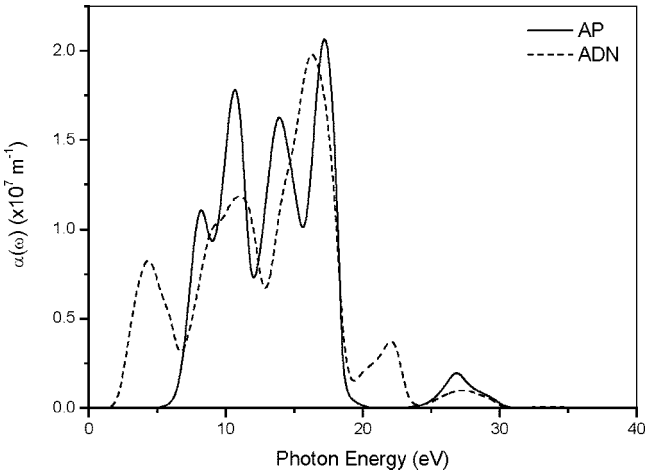

Figure 4. Optical absorption coefficient $\alpha(\omega)$ of crystalline AP and ADN.

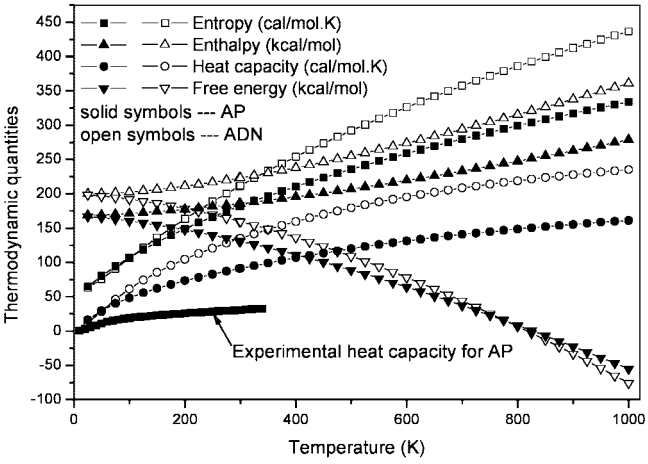

Figure 5. Thermodynamic properties of crystalline AP and ADN as a function of temperature.

at 8.17 eV corresponds to the breathing frequency of the perchlorate ion. The bands in the range 10.6−17.1 eV overlap forming the strongest absorption region that corresponds to distortion of the perchlorate ion. The peak at 26.9 eV corresponds to NH_4^+ deformation. Similarly, these peaks in absorption spectra of ADN reveal its structure and bonding. The absorption peak at 4.38 eV corresponds to the breathing frequency of the dinitramide ion. The bands in the range 11.1−16.3 eV overlap forming the strongest absorption region that corresponds to distortion of the dinitramide ion. The peak at 22.2 eV corresponds to NH_4^+ deformation, while the band at 27.6 eV corresponds to N−H stretching. The calculated results here present that the absorption spectra of AP and ADN display a few, strong bands in the fundamental absorption region, showing the two crystals have strong ionic bonding.

3.5. Thermodynamic Properties. In this section, the thermodynamic functions including enthalpy, entropy, free energy, and heat capacity for AP and ADN are evaluated and presented in Figure 5. We also compare the calculated heat capacity of AP with available experimental data[29] in Figure 5. Qualitatively, our calculations reproduce the evolution pattern of the experimental heat capacity with increasing temperature. The discrepancies may be due to different states of samples as well as different conditions of measurements in the experiments. We should note that our calculations are performed on the ordered structures but the experimental samples may be mixed by different phases, so the direct comparison between the calculated

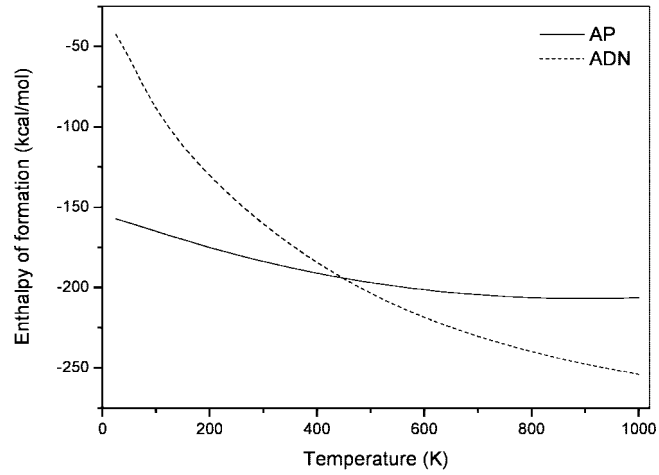

Figure 6. Enthalpy of formation for crystalline AP and ADN as a function of temperature.

and the measured results is difficult. However, our results should still be useful as references for experimental work. With the increase of temperature, the calculated enthalpies of crystalline AP and ADN monotonically increase; moreover, the enthalpy for ADN is greater than that for AP. This is because the main contributions to the enthalpy are from the translations and rotations of the molecules at lower temperature, whereas the vibrational motion is intensified at higher temperature and makes more contributions to the enthalpy. The same is true of the entropy and heat capacity. From the above-calculated vibrational properties, it is found that ADN has the larger vibrational motion modes of the frequencies than AP from the low frequency to high frequency region. Therefore, as the temperature increases, the vibrational motions of ADN make more contributions to the enthalpy, entropy, and heat capacity than these of AP. This leads to ADN having higher enthalpy, entropy, and heat capacity values than AP. For the free energy, the case is quite the contrary. As the temperature increases, the free energy values of AP and ADN gradually decrease; moreover, the free energy versus temperature curve of ADN crosses that of AP at about 780 K.

On the basis of the calculated thermodynamic functions, the enthalpy of formation and the free energy of formation can be evaluated. Concerning the formation energy, we consider the stabilities of AP and ADN with respect to decomposition reactions 2 and 3, respectively.

$$NH_4ClO_4 \rightarrow 1/2N_2 + 3/2H_2O + HCl + 5/4O_2 \quad (2)$$

$$NH_4N(NO_2)_2 \rightarrow 2NO + N_2 + 2H_2O \quad (3)$$

The calculated enthalpy and free energy of formation for AP and ADN are shown in Figures 6 and 7, respectively. It can be seen that the enthalpies of formation for AP and ADN become more and more negative with increasing temperature. This shows that the primary fission reactions are endothermic. In addition, we note that the enthalpy of formation versus temperature curve of AP crosses that of ADN at about 450 K. It is found from Figure 7 that the free energy of formation for AP and that for ADN are negative in the whole temperature range; moreover, the free energy of formation for ADN is greater than that for AP. This shows that the decomposition reactions 2 and 3 are more and more favorable as the temperature increases; moreover, ADN is easier to decompose than AP. In fact, the decomposition of AP occurs below approximately 300 °C,[3] whereas ADN decomposes at about 93.5 °C.[6]

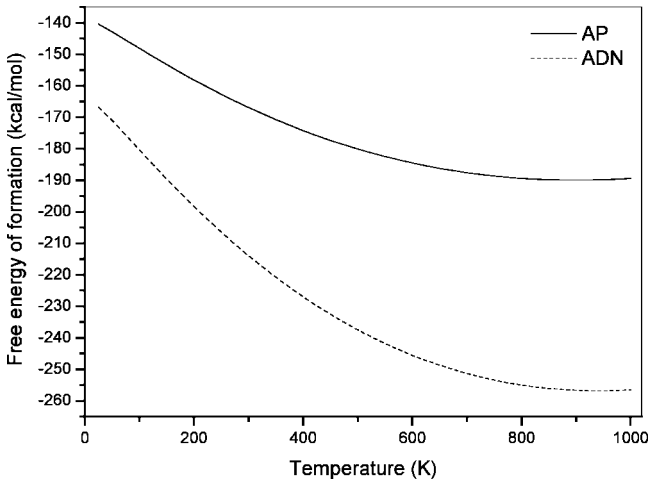

Figure 7. Free energy of formation for crystalline AP and ADN as a function of temperature.

4. Conclusions

In this study, we have performed a comparative DFT study of the electronic structure, vibrational properties, absorption spectra, and thermodynamic properties of crystalline AP and ADN in the local density approximation. The results shows that the p states for the two solids play a very important role in their chemical reaction. From the low frequency to high frequency region, ADN has more motion modes for the vibrational frequencies than AP. The motions of the NO_2 groups in ADN are diffusely distributed. The absorption spectra of AP and ADN display a few, strong bands in the fundamental absorption region, showing that the two crystals have strong ionic bonding. The thermodynamic properties show that the decomposition reactions of AP and ADN are more and more favorable as the temperature increases; moreover, ADN is easier to decompose than AP.

Acknowledgment. This work was partly supported by National Natural Science Foundation of China (Grant 10576016) and "973" Project. W.H.Z. is grateful for the funding from the School of Chemical Engineering and NJUST.

References and Notes

(1) Brill, T. B.; Budenz, B. T. *Progress in Aeronautics and Astronautics*, Vol. 185; Yang, V., Brill, T. B., Ren, W. Z., Eds.; American Institute of Aeronautics and Astronautics 2000; Chapter 1.1, pp 3–32.
(2) Politzer, P.; Lane, P. *J. Mol. Strut.* **1998**, *454*, 229.
(3) Jacobs, P. W. M.; Whitehead, H. M. *Chem. Rev.* **1969**, *69*, 551.
(4) Rossi, M. J.; Bottaro, J. C.; McMillen, D. F. *Int. J. Chem. Kinet.* **1993**, *25*, 549.
(5) Brill, T. B.; Brush, P. J.; Patil, D. G. *Combust. Flame* **1993**, *92*, 178.
(6) Vyazovkin, S.; Wight, C. A. *J. Phys. Chem. A* **1997**, *101*, 7217.
(7) Fetherolf, B. L.; Litzinger, T. A. *Combust. Flame* **1998**, *114*, 515.
(8) Sorescu, D. C.; Thompson, D. L. *J. Phys. Chem. B* **1999**, *103*, 6774.
(9) Sorescu, D. C.; Thompson, D. L. *J. Phys. Chem. A* **2001**, *105*, 7413.
(10) Payne, M. C.; Teter, M. P.; Allan, D. C.; Arias, T. A.; Joannopoulos, J. D. *Rev. Mod. Phys.* **1992**, *64*, 1045.
(11) Vanderbilt, D. *Phys. Rev. B* **1990**, *41*, 7892.
(12) Kresse, G.; Furthmüller, J. *Phys. Rev. B* **1996**, *54*, 11169.
(13) Fischer, T. H.; Almlof, J. *J. Phys. Chem.* **1992**, *96*, 9768.
(14) Ceperley, D. M.; Alder, B. J. *Phys. Rev. Lett.* **1980**, *45*, 566.
(15) Perdew, J. P.; Zunger, A. *Phys. Rev. B* **1981**, *23*, 5048.
(16) Peyronel, G.; Pignedoli, A. *Acta Crystallogr. Sect. B* **1975**, *31*, 2052.
(17) Gilardi, R.; Flippen-Anderson, J.; George, C.; Butcher, R. J. *J. Am. Chem. Soc.* **1997**, *119*, 9411.
(18) Sanchez-Portal, D.; Artacho, E.; Soler, J. M. *Solid State Commun.* **1995**, *95*, 685.
(19) Segall, M. D.; Shah, R.; Pickard, C. J.; Payne, M. C. *Phys. Rev. B* **1996**, *54*, 16317.
(20) Gonze, X. *Phys. Rev. B* **1997**, *55*, 10337.
(21) Bircumshaw, L. L.; Newman, B. H. *Proc. Roy. Soc. A* **1954**, *227*, 115.
(22) Vyazovkin, S.; Wight, C. A. *J. Phys. Chem. A* **1997**, *101*, 5653.
(23) Chakraborty, T.; Khatri, S. S.; Verma, A. L. *J. Chem. Phys.* **1986**, *84*, 7018.
(24) Prask, H. J.; Choi, C. S.; Chesser, N. J. *J. Chem. Phys.* **1988**, *88*, 5106.
(25) Russell, T. P.; Piermarini, G. J.; Block, S.; Miller, P. J. *J. Phys. Chem.* **1996**, *100*, 3248.
(26) Kirin, D.; Volovsek, V. *J. Chem. Phys.* **1997**, *106*, 9505.
(27) Saha, S.; Sinha, T. P.; Mookerjee, A. *Phys. Rev. B* **2000**, *62*, 8828.
(28) Isbell, R. A.; Brewster, M. Q. *Propell. Explos. Pyrot.* **1998**, *23*, 218.
(29) Westrum, E. F., Jr; Justice, B. H *J. Chem. Phys* **1969**, *50*, 5083.

JP800693E